Proceedings of the XII Serbian-Bulgarian Astronomical Conference (XII SBAC) Sokobanja, Serbia, September 25-29, 2020
Editors: L. Č. Popović, V. A. Srećković, M. S. Dimitrijević and A. Kovačević
Publ. Astron. Soc. "Rudjer Bošković" No 20, 2020, 61-68

STUDY OF THE FRACTAL DIMENSIONS IN THE MOLECULAR CLOUD ROSETTE BY USE OF DENDROGRAM ANALYSIS

MARIYANA BOGDANOVA, ORLIN STANCHEV and TODOR V. VELTCHEV

Department of Astronomy, University of Sofia, James Bourchier Blvd. 5, Sofia 1164, Bulgaria
E-mail: mpetrova@phys.uni-sofia.bg, o_stanchev@phys.uni-sofia.bg, eirene@phys.uni-sofia.bg

Abstract. The observed hierarchical structure in star-forming regions can be traced in terms of the fractal dimension. The latter is often defined as D=log N / log L where N is the number of fragments at given level and L is the scaling factor to the upper level. Such approach requires appropriate clump-extraction technique. An alternative approach is to explore the power-law exponent D_M of the mass-size relationship $\log(M) \propto D_M \log(L)$ where the scales L are defined in an abstract way (Beattie et al. 2019). We propose a method to derive this mass dimension D_M by use of the clump extraction technique DENDROGRAM (Rosolowsky et al. 2008). The method is applied to samples of dendrogram objects from integrated-intensity maps of ^{12}CO and ^{13}CO emissions and to dust-emission *(Herschel)* maps of the molecular cloud Rosette. The obtained scaling dependence of D_M is in general agreement with the numerical study of Beattie et al. (2019) for typical Mach numbers in molecular clouds and hints at the multifractal structure of Rosette.

1. INTRODUCTION

Observational studies of molecular clouds (MCs) in star-forming regions reveal complex sets of substructures: sheets, clumps, filaments and cores. Analysis of high-resolution maps shows that the filaments often contain dense prestellar cores of size ~0.1 pc (Andre et al. 2014) while most of the larger clumps are further decomposed to embedded condensations (see Bergin and Tafalla 2007, for review). This hierarchical, fractal cloud structure is crucial for understanding of the star formation process. Often used approaches to quantify it are studies of relationships mass *vs*. size and velocity dispersion *vs*. size in a power-law form interplay (Larson 1981, Heyer and Brunt 2004, Heyer et al. 2009) or derivation of

the fractal dimension in the cloud (Elmegreen and Falgarone 1996, Elmegreen 1997).

The choice of clump-finding method may influence significantly the analysis of fractal structure – whether clumps are considered as a set of independent objects or as a hierarchy in the position-position (PP) and/or in the position-position-velocity (PPV) space. In the latter case, clump properties can be linked to the general physics of star-forming regions. A widely used hierarchical clump-finding method is the DENDROGRAM technique (Rosolowsky et al. 2008) which is appropriate for study of the fractal structure of MCs.

In this report we present a method for derivation of fractal dimensions in MCs based on their dendrogram structure derived from integrated-intensity and column-density (PP) maps. The object chosen to test the method is the Rosette MC.

2. OBSERVATIONAL DATA ON THE MOLECULAR CLOUD ROSETTE

We make use of ^{12}CO/^{13}CO maps (PPV cubes) taken with the 14 m telescope of Five College Radio Astronomy Observatory (FCRAO), presented and discussed by Heyer, Williams and Brunt (2006). Angular resolution of 46 arcsec allows for study of structures with sizes greater than ~0.15 pc (adopting distance to Rosette MC of 1.33 kpc, Lombardi, Alves and Lada 2011).

From the row PPV cubes we construct PP integrated-intensity maps. The process contains extraction of the channels that contain only noise, calculation of the noise levels for the rest of the channels and integration over the V axis for them. The maps of dust emission were obtained from *Herschel* observations at four wavelengths of PACS and SPIRE: 160, 250, 350, and 500 μm (see Schneider et al. 2010, 2012, for details) and convolved to a common angular resolution of 36 arcsec.

The star-forming Rosette is appropriate as a test object because of its intensive investigation in the last decades. Its local structure have been studied using various algorithms and tracers (Williams et al. 1995; Schneider et al. 1998; Dent et al. 2009; Di Francesco et al. 2010; Veltchev et al. 2018).

3. SELECTED SAMPLES OF THE DENDROGRAM METHOD

The DENDROGRAM technique (Rosolowsky et al. 2008), implemented in the Python library ASTRODENDRO, constructs two-dimensional map of the hierarchical cloud structure. The largest object of the hierarchy is called *root.* Each node in the dendrogram tree splits to exactly two substructures and a sequence of nodes is called *branch*. At the top of each branch are two *leaves* (associated with intensity maxima): objects without substructures.

We compose dendrogram trees in Rosette varying two input parameters of the technique (Fig. 1). Lower intensity limit T_0 (in units K) defines the level above which extraction of the trunk is allowed and, hence, sets up the largest scale in the

tree. The second input parameter ΔT_{max} represents the minimal intensity difference between the level of a node and the levels of its *both* substructures (Fig. 1). We vary T_0 and ΔT_{max} in order to select samples of dendrogram objects which: i) are rich enough; and ii) are free of objects associated with `spikes' due to noise. The chosen T_0 is different for different tracers in view of their various noise levels. Variation of ΔT_{max} controls the number of structures – decreasing the value of this parameter leads to extraction of more structures.

We chose $T_0 = 1$ for the ^{12}CO map and $T_0 = 2$ for the ^{13}CO and dust maps. The authors of the DENDROGRAM technique do not recommend values $\Delta T_{max} < 2$ in order to avoid the noise `spikes'. We opt for $\Delta T_{max} = 1$ only for the *Herschel* map – due to the low number of substructures and the need of better statistics for our method. It should be pointed out also, that the noise values in this case are low.

The samples of dendrogram objects selected for derivation of fractal dimensions are:

- ^{12}CO : $T_0 = 1$, $\Delta T_{max} = 2$ (369 objects)
- ^{13}CO : $T_0 = 2$, $\Delta T_{max} = 3$ (2075 objects)
- Dust: $T_0 = 2$, $\Delta T_{max} = 1$ (144 objects)

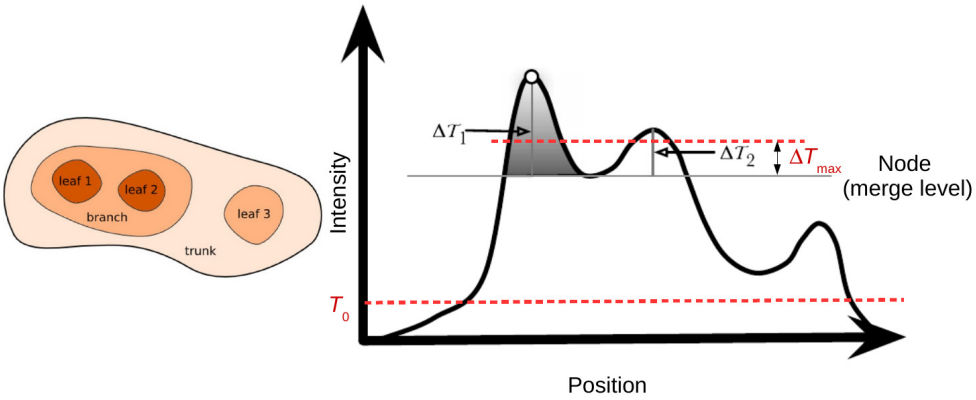

Figure 1: On the construction of the dendrogram tree from an integrated intensity map and the choice of the parameters T_0 and ΔT_{max} (see text). Only bifurcations with $\Delta T_1 > \Delta T_{max}$ and $\Delta T_2 > \Delta T_{max}$ are identified as nodes; the first such node with $T > T_0$ is identified as the root of the tree.

4. APPROACH TO DERIVE MASS DIMENSION D_M

Various approaches to calculate fractal dimensions for different structures are found in the literature. Most of them are essentially geometrical, e.g. the classical dimension of 3D fractals $D_f = \log N / \log S$, where N is the number of substructures at given scale and $S > 1$ is the scaling factor (Elmegreen, 1997;

Sánchez et al., 2005), and the box-counting dimension D_{BC}, which measures the coverage of the hierarchical object by grids of decreasing box size. Such methods account rather for geometrical properties and not for the physics behind the observed hierarchical structure properties of the objects.

More reliable approaches to describe the fractal structure of MCs are methods for derivation of the so-called *mass-length dimension* D_M, defined as the power-law exponent of the mass-size relation $M \propto L^{D}$ (Mandelbrot, 1983). Such a method was applied by Beattie et al. (2019, hereafer, BFK), using surface-density map of simulated turbulent MCs without self-gravity. The length scales in their approach are defined as increasing sizes of embedded boxes starting from a chosen peak (Fig. 2, left).

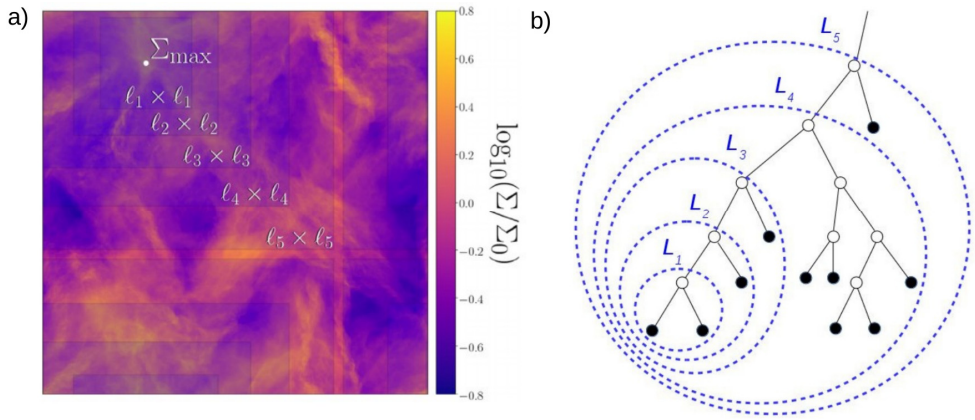

Figure 2: Comparison between two approaches to derive D_M from integrated-intensity (or column-density) maps: a) BFK (see Fig. 2 there); b) this report. See text for details.

We suggest a method to derive the fractal dimensions D_M which is similar to that of BFK but designed to be applied to a dendrogram tree. A pair of leaves (associated with some local integrated-intensity peaks) and the node they belong to are taken as the bottom of a sequence of length scales $L_1 < L_2 < \ldots < L_n$ where each L_i is the effective size of a node in the chosen branch of the dendrogram tree (Fig. 2, right) and $L_n = L_{max}$ is the effective size of the root (which depends on the choice of the input parameter T_0). The fractal dimension $D_M(L_i)$ at given scale L_i is calculated as the slope of power-law fit performed on the data set $[(L_i, M_i);(l_j, m_j)]$ where (l_j, m_j) are the sizes and masses of all substructures included in the node (L_i, M_i), i.e. of all objects within the corresponding dashed blue line in Fig. 2, right. In that way the method takes into account the contribution of the other branch that merges with the traced one in given node of size L_i.

5. SCALE DEPENDENCE OF D_M IN ROSETTE

The results of our calculations from the ^{12}CO/^{13}CO maps are presented in Fig. 3. The length scales are normalized to the effective size L of the root in the chosen sample of dendrogram objects – this structure includes the whole star-forming region (on the ^{12}CO map) and only the Rosette MC + the Monoceros ridge (on the ^{13}CO map). The curves D_M=$D_M(l/L)$ derived by BFK for Mach numbers 1 (transition to transonic regime) and 20 (highly supersonic regime) are plotted for comparison.

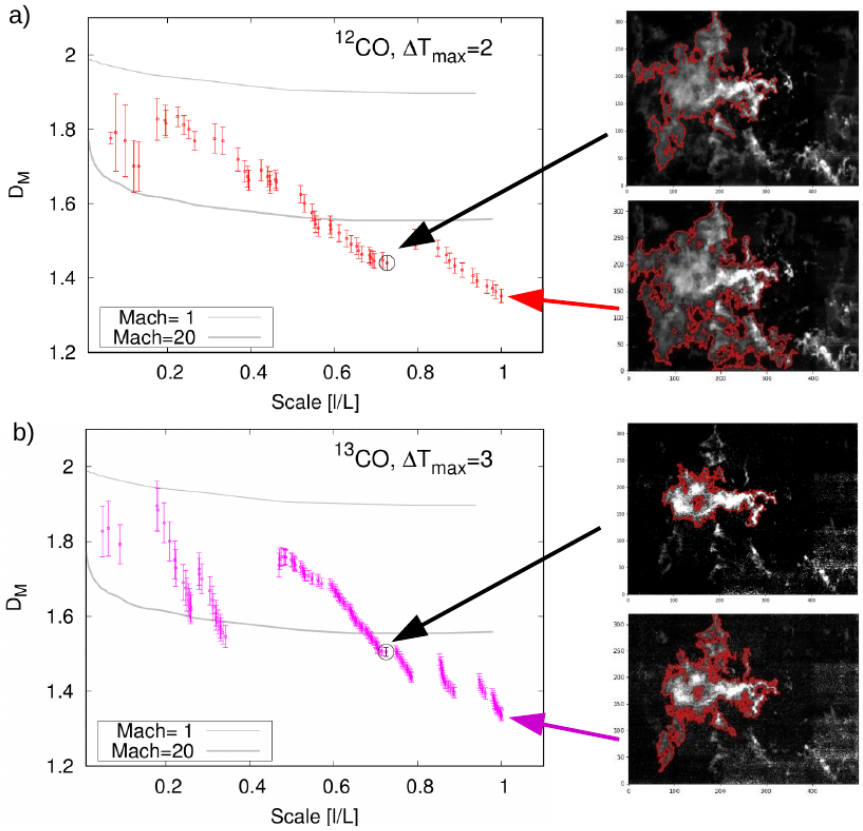

Figure 3: Scale dependence of D_M in the star-forming region Rosette as derived from: a) ^{12}CO maps; b) ^{13}CO maps. The largest scale (l=L) and the substructure which includes Rosette MC and the Monoceros ridge are shown with arrows.

In general, the derived scaling dependence of D_M from the ^{12}CO/^{13}CO maps (Fig. 3) is consistent with the numerical models of BFK in the scale range l/L<0.5. These dendrogram objects are mostly structures in the main ridge of the cloud which are probably not influenced by feedback effects (gas compression, heating) from the OB cluster NGC 2244 located in the bottom-right corner of the maps in

Fig. 3. At small scales (l/L<0.2) D_M~1.8, in broad agreement with the classical value D_M~2 found by Larson (1981) for a large sample of MCs and their substructures. At larger scales the derived values of D_M decrease quasi-monotonically in the ^{12}CO case and with notable discontinuities in the ^{13}CO case. The general trend hints at multifractal cloud structure. The difference between the scale dependences of D_M derived from the CO tracers can be attributed to the optical thickness of the ^{12}CO emission at high densities (Draine 2011). Thus ^{12}CO traces regions of lower column density and may fail to identify dense structures at small scales. Probably this is the reason for the smoother scale dependence of the fractal dimension from the ^{12}CO sample compared to ^{13}CO (Fig. 3).

There are at least two possible explanations of the inconsistency of our results at large scales (l/L~0.7 and larger) with the numerical study of BFK. First, the largest structures include zones outside the Rosette MC – mostly from the Monoceros Ridge – where the physical conditions differ substantially. Second, the number of dendrogram objects per bin in this scale range obviously increases which affects the output of the fitting procedure. Probably this is an artifact of the DENDROGRAM technique itself and needs to be clarified in a forthcoming study.

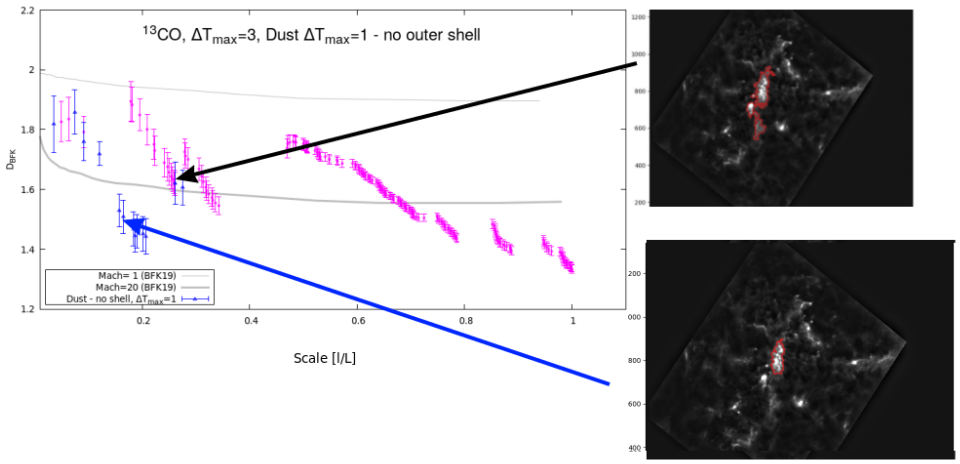

Figure 4: Scale dependence of D_M in Rosette MC derived from *Hershel* maps compared with the results from ^{13}CO maps. Structures in the main ridge of the cloud are shown with arrows.

In Fig. 4 we compare the scale dependence of D_M derived from the *Hershel* maps with the results from the ^{13}CO tracer. Dust emission is optically thin which allows investigation of denser fragments of the Rosette MC as seen on the map (Fig. 4, right). Unfortunately, the sample size is small and this affects significantly the derivated values of D_M. The smallest dust structures yield fractal dimensions in agreement with the results from the ^{12}CO/^{13}CO samples while the discontinuity of the scale dependence of D_M is probably an effect of the sample size.

6. CONCLUSION

We suggest a method to estimate the fractal dimensions D in molecular clouds by use of the mass-size relation $M(L) \sim L^{-D}$ where the power index $D=D_M$ is called mass-length dimension. In contrast to the similar approach of Beattie et al. (2019), the technique is not based on abstract scales but deals with samples of dendrogram objects with their effective sizes.

The star-forming region Rosette was chosen as an object to test the method, by use of maps in molecular-line (^{12}CO/^{13}CO) and dust-emission tracers. The derived scale dependence of D_M in Rosette MC is in general agreement with the numerical study of Beattie et al. (2019) for molecular clouds in transonic up to highly supersonic regime. The inconsistency found at larger scales which correspond to the whole star-forming region could be explained by changes in the physical conditions and/or with artifacts of the DENDROGRAM technique. This needs to be clarified in a forthcoming study.

Acknowledgements

The authors are grateful to M. Heyer and J. Williams for the FCRAO molecular-line maps and to N. Schneider for the *Herschel* maps of Rosette given at our disposal and used in this report.

M. Bogdanova thanks to the Bulgarian National Science Fund for providing support through Grant KP-06-PM-38/6 (Fundamental research by young scientists and postdocs 2019). T. Veltchev acknowledges funding from the Ministry of Education and Science of the Republic of Bulgaria, National RI Roadmap Project DO1-277/16.12.2019.

References

Andre P. et al.: 2010, *Astronomy & Astrophysics*, 518, L102.

André P., Di Francesco J., Ward-Thompson D., Inutsuka S.-I., Pudritz R., Pineda J.: 2014, in Beuther H., Klessen R. S., Dullemond C., Henning T., eds, *Protostars and Planets VI*. Univ. Arizona Press, Tucson, p. 27.

Beattie J., Federrath C., Klessen R. S.: 2019, *Monthly Notices of the Royal Astronomical Society*, 487, 2070 (BFK).

Bergin E. A., Tafalla M.: 2007, *Annual Review of Astronomy and Astrophysics* , 45, 339.

Dent W. et al.: 2009, *Monthly Notices of the Royal Astronomical Society*, 395, 1805.

Di Francesco J. et al.: 2010, *Astronomy & Astrophysics*, 518, L91.

Draine B.& 2011, *Physics of the Interstellar and Intergalactic Medium*. Princeton Univ. Press, Princeton, NJ.

Elmegreen B. G.: 1997, *The Astrophysical Journal*, 486, 944.

Elmegreen B. G., Falgarone E.: 1996, *The Astrophysical Journal*, 471, 816.

Heyer M., Brunt C.: 2004, *The Astrophysical Journal*, 615, L45.

Heyer M., Krawczyk C., Duval J., Jackson J.: 2009, *The Astrophysical Journal*, 699, 1092.

Heyer M., Williams J., Brunt C.: 2006, *The Astrophysical Journal*, 643, 956.

Larson R.: 1981, *Monthly Notices of the Royal Astronomical Society*, 194, 809.

Lombardi M., Alves J., Lada C.: 2011, *Astronomy & Astrophysics*, 535, A16.
Mandelbrot B. (1983). The Fractal Geometry of Nature. W. H. Freeman and Co., New York, United States of America. ISBN 0-7167-1186-9.
Rosolowsky E., Pineda J., Kauffmann J., Goodman A.: 2008, *The Astrophysical Journal*, 679, 1338.
Sánchez N., Alfaro E. J., & Pérez E.: 2005, *The Astrophysical Journal*, 625, 849.
Schneider N., Stutzki J., Winnewisser G., Block D.: 1998, *Astronomy & Astrophysics,* 335, 1049.
Schneider N., Motte F., Bontemps S., Hennemann M., et al.: 2010, *Astronomy & Astrophysics,* 518, L83.
Schneider N., Csengeri T., Hennemann M., Motte F., et al.: 2012, *Astronomy & Astrophysics*, 540, L11.
Veltchev T., Ossenkopf-Okada V., Stanchev O., Schneider N., Donkov S., Klessen R. S.: 2018, *Monthly Notices of the Royal Astronomical Society*, 475, 2215.
Williams J., Blitz L., Stark A.: 1995, *Astrophysical Journal*, 451, 252.